MOX–Report No. 14/2014

Degenerate Tetrahedra Recovering

Dassi, F.; Formaggia, L.; Zonca, S.

MOX, Dipartimento di Matematica "F. Brioschi"
Politecnico di Milano, Via Bonardi 9 - 20133 Milano (Italy)

mox@mate.polimi.it http://mox.polimi.it

Degenerate Tetrahedra Recovering

Franco Dassi[♯] and Luca Formaggia[♯] and Stefano Zonca[♯]

April 8, 2014

[♯] MOX– Modellistica e Calcolo Scientifico
Dipartimento di Matematica "F. Brioschi"
Politecnico di Milano
via Bonardi 9, 20133 Milano, Italy
franco.dassi@mail.polimi.it
luca.formaggia@mail.polimi.it
stefano.zonca@mail.polimi.it

Keywords: tetrahedral mesh mesh quality mesh adaptation.

Abstract

Many mesh generation or optimization algorithms could produce a low quality tetrahedral mesh, i.e. a mesh where the tetrahedra have very small solid or dihedral angles. In this paper, we propose a series of operations to recover these degenerate tetrahedra. In particular, we will focus on the standard shapes of these undesired mesh elements (sliver, cap, wedge and spade) and, for each of these configurations, we apply a suitable sequence of classical mesh modification procedures to get a higher quality mesh. The reliability of the proposed mesh optimization algorithm is numerically proved with some examples.

1 Introduction

Creating a "good quality" mesh is the main issue in mesh generation and optimization algorithms. In fact, the accuracy or the speed of a numerical simulation could be hampered by just a few "bad elements". Understanding what "bad" and "good" elements means and how to get a "good quality" mesh have become a central problem in this area.

In [12], it is shown that the concept of "good element" is strictly related to the application and the numerical methods employed. In a volume tetrahedral mesh, we could say that, in general, elements with very small solid and dihedral angles should be avoided, since they usually decrease the accuracy and the performance of a numerical methods.

We observe that if the mesh elements are aligned according to a precise criterion, e.g., the gradient of a finite element solution, they could lead to a better result than a mesh composed by equilateral elements, see, e.g., [5, 11, 8]. However, in this work we focus in obtaining “nearly isotropic” tetrahedral meshes, i.e., meshes where we avoid elements whose shape is too far from that of equilateral tetrahedron.

The literature is rich of optimization algorithms to improve the shape of the tetrahedral elements. In [6], Freitag and Knupp present a shape measure for tetrahedra moving from the condition number of the linear transformation between a unit equilateral tetrahedron and any tetrahedron. Thanks to this shape-measure, they formulate two optimization objective functions that aim at improving the worst-quality element in the mesh by a node-smoothing algorithm.

In [3] Edelsrunner and Guoy demonstrate that the so-called sliver exudation procedure is able to remove the majority of degenerate tetrahedra, but unfortunately some bad shaped tetrahedra still remain in the final mesh.

In [7] Freitag and Ollivier-Gooch propose a node smoothing procedure combined with a flipping algorithm to improve the shape of the tetrahedra of a mesh. In particular, they numerically show that these two operations are crucial to achieve a better quality mesh in a computationally efficient manner.

Even if the previous algorithms may produce excellent meshes composed by well shaped tetrahedra, they do not exploit all the possible local tetrahedral mesh operations and a few bad elements can remain. Indeed, a more aggressive set of operations should be applied to get even better result. This is the basic idea behind the optimization strategy proposed in [2, 1, 10]. In [2, 1] Acikgoz and Bottasso use a metric-driven mesh adaptation procedure. More in detail, in [2] Bottasso uses a standard Gauss-Seidel removal algorithm. Each element is visited and a series of attempt are made to remove these undesired elements and locally increase the mesh quality. These operations include different type of vertex insertion, edge contraction, flips and vertex smoothing. Unfortunately this approach produces clusters of bad elements. In [1] Acikgoz and Bottasso give a solution to this “frozen” cluster of elements by leaving the “greedy policy” of [2] and introducing a simulated annealing technique. The acceptance criterion of the previous down-hill greedy policy is now modified such that new local triangulations are accepted based on a probably function, which inserts randomness on the process. In [10], Klinger and Shewchuk do not use the metric, but they identify the low-quality tetrahedra and they apply a large variety of mesh operations to improve the mesh quality. Their results are really impressive, in fact they could get a final mesh with a very large minimum dihedral angle: about 38°. But, since they do not aim at optimizing the computational effort, this procedure is rather computationally inefficient.

This work is inspired by this last optimization procedure. In particular, we propose an optimization algorithm that applies a series of “ad-hoc” operations for each type of degenerate tetrahedra. Another important aspect is the speed: we set up an optimization procedure that is reasonably fast to be applied in practical situations.

The paper is organized as follow. In Section 2, we introduce the tetrahedral quality index and a new procedure to detect the different shape of degenerate elements. Then, in Section 3, we describe a vertex smoothing algorithm and the sequence of operations to recover each case of degeneration. Finally, in Section 4, we numerically show the reliability of both the degenerate element detection and the mesh improvement algorithm. Conclusions and future works are discussed in Section 5.

2 Tetrahedra Quality

In a mesh generation framework, it is necessary to define some precise criteria to evaluate the reliability of the tetrahedral elements. In particular, this criterion should be a single and easy-computed measure, in order to evaluate the "goodness" of an individual element, i.e., to estimate how far is the tetrahedral shape from the equilateral one.

There is not a unique quantity to evaluate this measure, see, e.g. [12]. The most general one is the so called aspect ratio.

Definition 1 *Consider a tetrahedron T, the* ***aspect ratio*** *is defined as:*

$$q_{as}(T) := \frac{l_{max}}{h_{min}}\,, \tag{1}$$

where l_{max} is the longest edge and h_{min} is the shortest height of the tetrahedron T. This quantity varies in $[\sqrt{2}/\sqrt{3}, +\infty)$, and values close to $\sqrt{2}/\sqrt{3}$ implies a better shape, i.e, the tetrahedron T is close to the equilateral one.

To have a quantity that varies in $[0, 1]$, we use the following normalized measure

$$q(T) := \frac{\sqrt{2}}{\sqrt{3}}\frac{1}{q_{\mathrm{as}}(T)}\,. \tag{2}$$

If the quantity $q(T)$ is close to 0, the tetrahedron T is not well shaped, i.e., it has very small or too large dihedral and solid angles. If $q(T)$ is close to 1, it means that the shape of the tetrahedron is close to the shape of the equilateral tetrahedron, i.e. a tetrahedron that has all the edges of the same length and the same dihedral and solid angles.

Definition 2 *Consider the finite set $S = \{T_1, T_2, \dots T_n\}$, where T_i is a tetrahedron $\forall i = 1, 2, \dots n$. We define the quality of S as*

$$q(S) := \min_{T_i \in S} q(T_i)\,. \tag{3}$$

2.1 Detection of Degenerate Tetrahedra

There are different types of degenerate tetrahedra, characterized by a different shape. Unfortunately the quality indexes proposed in literature, [12], just detect that they have a bad shape, but they do **not** distinguish the various cases reported in Figure 1.

The proposed mesh optimization procedure applies different strategies according to these undesired configurations, in order to improve the quality of the whole mesh. Consequently, we can not use only the quality index defined in Equation (2), but we have to proceed with a deeper analysis on the shape of the tetrahedra. Before dealing with this issue, we recall some useful definitions and results.

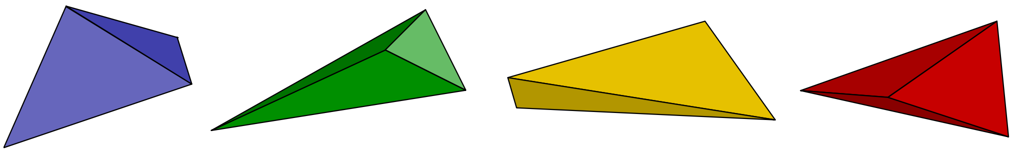

Figure 1: Different types of degenerate tetrahedra.

Definition 3 *The **barycentric coordinates** of a point $\boldsymbol{p}$ related to a finite set of point $S = \{\boldsymbol{v}_1, \boldsymbol{v}_2, \ldots \boldsymbol{v}_n\}$ are the coefficients $\mu_i \in \mathbb{R}$ such that*

$$\boldsymbol{p} = \sum_{i=1}^{n} \mu_i \boldsymbol{v}_i \,. \tag{4}$$

Definition 4 *Consider a triangle $\boldsymbol{v}_1\boldsymbol{v}_2\boldsymbol{v}_3$ whose vertexes are given with a specific order and whose area is A. The **signed area** is defined as*

$$|\boldsymbol{v}_1\boldsymbol{v}_2\boldsymbol{v}_3| := \begin{cases} A & \textit{if the vertexes follow a clockwise order} \\ -A & \textit{if the vertexes follow a counter clockwise order} \end{cases} . \tag{5}$$

Proposition 2.1 *Consider a triangle $\boldsymbol{v}_1\boldsymbol{v}_2\boldsymbol{v}_3$ and a point $\boldsymbol{p}$ that lies on the plane defined by $\boldsymbol{v}_1\boldsymbol{v}_2\boldsymbol{v}_3$. The barycentric coordinates of $\boldsymbol{p}$ could be computed by the formula*

$$\mu_{\boldsymbol{v}_1} = \frac{|\boldsymbol{p}\boldsymbol{v}_2\boldsymbol{v}_3|}{|\boldsymbol{v}_1\boldsymbol{v}_2\boldsymbol{v}_3|} \quad \mu_{\boldsymbol{v}_2} = \frac{|\boldsymbol{v}_1\boldsymbol{p}\boldsymbol{v}_3|}{|\boldsymbol{v}_1\boldsymbol{v}_2\boldsymbol{v}_3|} \quad \mu_{\boldsymbol{v}_3} = \frac{|\boldsymbol{v}_1\boldsymbol{v}_2\boldsymbol{p}|}{|\boldsymbol{v}_1\boldsymbol{v}_2\boldsymbol{v}_3|} \,. \tag{6}$$

Remark 1 *Consider a triangle $\boldsymbol{v}_1\boldsymbol{v}_2\boldsymbol{v}_3$ and a point $\boldsymbol{p}$ on the plane identified by $\boldsymbol{v}_1\boldsymbol{v}_2\boldsymbol{v}_3$. The barycentric coordinates of $\boldsymbol{p}$ are proportional to the ratio between the heights of the triangles **pbc**, **apc** and **abp** respect to the height of $\boldsymbol{v}_1\boldsymbol{v}_2\boldsymbol{v}_3$.*

Proof. We consider the triangle $\mathbf{v}_1\mathbf{v}_2\mathbf{v}_3$ and the barycentric coordinates of $\mathbf{p}$ related to the vertex $\mathbf{v}_1$, $\mu_{\mathbf{v}_1}$. The triangles $\mathbf{p}\mathbf{v}_2\mathbf{v}_3$ and $\mathbf{v}_1\mathbf{v}_2\mathbf{v}_3$ have a common edge, $\mathbf{v}_2\mathbf{v}_3$. We consider the heights $h_{\mathbf{p}}$ and $h_{\mathbf{v}_1}$ related to the base $\mathbf{v}_2\mathbf{v}_3$ of the triangles $\mathbf{p}\mathbf{v}_2\mathbf{v}_3$ and $\mathbf{v}_1\mathbf{v}_2\mathbf{v}_3$, respectively. Without loss of generality, we could consider that both $|\mathbf{p}\mathbf{v}_2\mathbf{v}_3|$ and $|\mathbf{v}_1\mathbf{v}_2\mathbf{v}_3|$ is positive, then the following chain of equalities holds

$$\mu_{\mathbf{v}_1} = \frac{|\mathbf{p}\mathbf{v}_2\mathbf{v}_3|}{|\mathbf{v}_1\mathbf{v}_2\mathbf{v}_3|} = \frac{\frac{1}{2}h_{\mathbf{p}}l_{\mathbf{v}_2\mathbf{v}_3}}{\frac{1}{2}h_{\mathbf{v}_1}l_{\mathbf{v}_2\mathbf{v}_3}} = \frac{h_{\mathbf{p}}}{h_{\mathbf{v}_1}} \quad \Rightarrow \quad h_{\mathbf{p}} = \mu_{\mathbf{v}_1}h_{\mathbf{v}_1} \,,$$

where $l_{\mathbf{v}_2\mathbf{v}_3}$ is the length of the base $\mathbf{v}_2\mathbf{v}_3$. We can repeat the same computation for each barycentric coordinates and this complete the proof.

□

Remark 2 *Consider the plane π identified by $\boldsymbol{v}_1\boldsymbol{v}_2\boldsymbol{v}_3$, it is possible to represent each point of the plane π via the barycentric coordinates of $\boldsymbol{p}$ associated with the triangle $\boldsymbol{v}_1\boldsymbol{v}_2\boldsymbol{v}_3$.*

Consider a tetrahedron T, whose vertexes are the points $\mathbf{v}_1$, $\mathbf{v}_2$, $\mathbf{v}_3$ and $\mathbf{v}_4$. If T has a quality index lower than a threshold value, see Subsection 4.1, we analyze more in detail its shape. More precisely, we consider the face associated with the greatest area, let say $\mathbf{v}_1\mathbf{v}_2\mathbf{v}_3$, then we project point $\mathbf{v}_4$ on the plane π identified by $\mathbf{v}_1\mathbf{v}_2\mathbf{v}_3$. According to the position of this projection, we are able to identify which type of "bad shape" we are dealing with via the barycentric coordinates of this projection related to the triangle $\mathbf{v}_1\mathbf{v}_2\mathbf{v}_3$. In fact, the plane π is partitioned in the following regions:

$$
\begin{aligned}
\Omega_{\text{sliver}} &:= \{\exists i \in \mathcal{I} : \mu_i < -\delta\}\,,\\
\Omega_{\text{cap}} &:= \{\forall i \in \mathcal{I} : \delta < \mu_i < 1\}\,,\\
\Omega_{\text{spade}} &:= \{\exists i \in \mathcal{I} : 0 < \mu_i < \delta\,, \forall j \neq i,\, j \in \mathcal{I}\,, \mu_j > \delta\}\,,\\
\Omega_{\text{wedge}} &:= \{\exists i \in \mathcal{I} : \delta < \mu_i < 1\,, \forall j \neq i,\, j \in \mathcal{I}\,, -\delta < \mu_j < \delta\}\,,
\end{aligned}
$$

where $\mathcal{I} := \{1,\, 2,\, 3\}$, $\mu_{\mathbf{v}_1}$, $\mu_{\mathbf{v}_2}$ and $\mu_{\mathbf{v}_3}$ are the barycentric coordinates associated with the triangle $\mathbf{v}_1\mathbf{v}_2\mathbf{v}_3$ and δ is a threshold value, see Subsection 4.1. Consequently, if the projection of $\mathbf{v}_4$ on π, $\mathbf{v}_4'$, is inside of one of these regions, we have identified the kind of "bad shape". For instance, if $\mathbf{v}_4' \in \Omega_{\text{sliver}}$, the corresponding tetrahedron is a sliver.

Remark 3 *The parameter δ used in the definition of the domains Ω_{sliver}, Ω_{cap}, Ω_{spade} and Ω_{wedge} measures how far $\boldsymbol{v}_4'$ is from an edge of the triangle $\boldsymbol{v}_1\boldsymbol{v}_2\boldsymbol{v}_3$.*

Proof. This is a simple observation that cloud be easily proved via Remark 1.

□

3 Recover Degenerate Tetrahedron

In this section we describe more in detail the mesh operations applied to improve the mesh quality. These operations could be divided into two main categories:

- *global operations:* we apply a node-smoothing on the mesh vertexes to globally improve the quality of the mesh without changing its topology;
- *local specific operations:* we have implemented a series of local mesh operations such as vertex insertion and edge contraction, specific for each degenerate tetrahedron.

3.1 Vertex Smoothing

Smoothing is one of the classical method to modify a mesh. For a given vertex $\mathbf{v}$, the smoothing operation consists in finding a new location for this vertex such that the local mesh quality is improved **without** changing the mesh topology.

This new position could bring to invalid configuration such as inverted tetrahedra. Indeed, once a vertex is moved, a check on the validity of the new mesh has to be performed.

In this paper we use a classical smoothing for tetrahedral mesh, [9]. Consider a point $\mathbf{v}$ and the set of tetrahedra connected to this point, $\omega_{\mathbf{v}}$. We move the point $\mathbf{v}$ in the barycenter of the volume identified by $\omega_{\mathbf{v}}$, i.e.,

$$\mathbf{v}' = \frac{1}{V_{\omega_{\mathbf{v}}}} \int_{\omega_{\mathbf{v}}} \mathbf{x} \, dV \,, \tag{7}$$

where $V_{\omega_{\mathbf{v}}}$ denotes the volume of $\omega_{\mathbf{v}}$ and $\mathbf{v}'$ is the barycenter of $\omega_{\mathbf{v}}$.

Remark 4 *Consider a point on the hull or on an interface of the volume,* $\mathbf{w}$*. Since the barycenter of* $\omega_{\mathbf{w}}$ *does not lie on the hull, if we move* $\mathbf{w}$ *in this new location, we could not preserve the volume of the mesh. To avoid this issue, we do not move the points that lie on the hull or the interface.*

3.2 Composite Operations for Degenerate Tetrahedra

In this subsection we present the sequence of operations applied on the different types of degenerate tetrahedra. This is the actual novelty of the proposed mesh optimization procedure. In the following paragraph we consider a tetrahedron $\mathbf{v}_1\mathbf{v}_2\mathbf{v}_3\mathbf{v}_4$ that has a quality index $q < q_{\text{min}}$, see Section 2, and we suppose that the face associated with the maximum area is $\mathbf{v}_1\mathbf{v}_2\mathbf{v}_3$.

Sliver. Suppose that the tetrahedron $\mathbf{v}_1\mathbf{v}_2\mathbf{v}_3\mathbf{v}_4$ is a sliver. To improve the quality of the mesh, we proceed as follow. We consider the two edges $e_1 = \mathbf{v}_1\mathbf{v}_2$ and $e_2 = \mathbf{v}_3\mathbf{v}_4$ associated with the maximum dihedral angles, see Figure 2 (a). We split both these edges into their middle points, $\mathbf{m}_1$ and $\mathbf{m}_2$, see Figure 2 (b), then we contract the new edge $\mathbf{m}_1\mathbf{m}_2$ onto its middle point, $\mathbf{w}$, see Figure 2 (c). Then, we try to contract the edges $\mathbf{w}\mathbf{v}_i$ onto $\mathbf{v}_i$ for $i = 1, 2, 3, 4$. If more than one of these contractions do not produce any inverted tetrahedra, we consider the configuration that produces a higher quality mesh. More in detail, let S be the set of tetrahedra connected to $\mathbf{v}_1\mathbf{v}_2\mathbf{v}_3\mathbf{v}_4$ and let S_i the set of tetrahedra after the contraction of the edge e_i, we contract the edge e_i related to the maximum value of $q(S_i)$, see Definition 2.

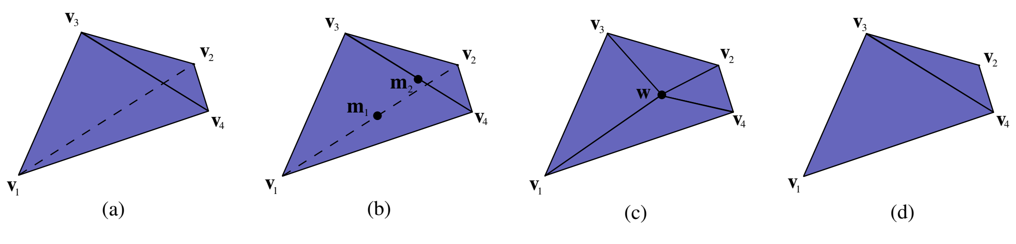

Figure 2: Procedure in the case of sliver. In (d) the faces that could remain in the tetrahedral mesh.

Cap. Suppose that the tetrahedron $\mathbf{v}_1\mathbf{v}_2\mathbf{v}_3\mathbf{v}_4$ is a cap, Figure 3 (a). To remove this degenerate element, we contract one of the edges $e_1 = \mathbf{v}_1\mathbf{v}_4$, $e_2 = \mathbf{v}_2\mathbf{v}_4$ or $e_3 = \mathbf{v}_3\mathbf{v}_4$, onto the vertex $\mathbf{v}_1$, $\mathbf{v}_2$ or $\mathbf{v}_3$, respectively, see Figure 3 (b).

If more than one of these collapses does not produce any inverted tetrahedron, we remove the edge whose contraction is associated with the resulting highest quality of the tetrahedra involved. More precisely, let S be the set of tetrahedra connected to $\mathbf{v}_1\mathbf{v}_2\mathbf{v}_3\mathbf{v}_4$ and let S_i the set of tetrahedra after the contraction of the edge e_i, we contract the edge e_i related to the maximum value of $q(S_i)$, see Definition 2.

In the case that none of the contractions is possible we proceed with a classical 2-3 flip of the face $\mathbf{v}_1\mathbf{v}_2\mathbf{v}_3$. Even if the 2-3 flip is not allowed, we leave this degenerate tetrahedron.

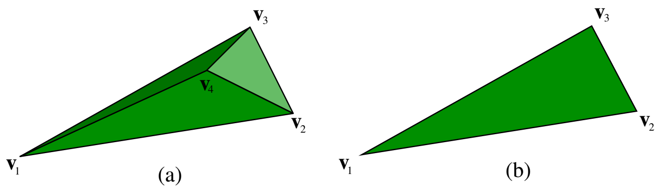

Figure 3: Procedure in the case of cap. In (b) the faces that could remain in the tetrahedral mesh.

Wedge. Suppose that the tetrahedron $\mathbf{v}_1\mathbf{v}_2\mathbf{v}_3\mathbf{v}_4$ is a wedge, see Figure 4 (a). We consider its shortest edge $e = \mathbf{v}_1\mathbf{v}_2$, and we try to contract it in one of its endpoints or onto its middle point, see Figure 4 (b). If more than one of these contractions does not produce any inverted tetrahedron, we consider the set of tetrahedra S involved in the contraction of e onto the node that maximize the quality of S, see Definition 2. In the case that none of these operations is possible, we leave this degenerate tetrahedron.

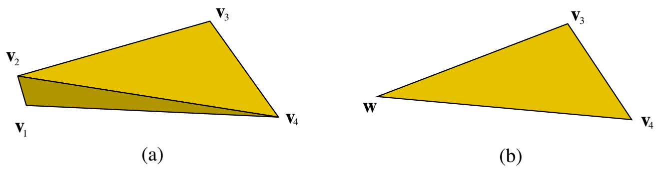

Figure 4: Procedure in the case of wedge. In (b) the faces that could remain in the tetrahedral mesh.

Spade. Suppose that the tetrahedron $\mathbf{v}_1\mathbf{v}_2\mathbf{v}_3\mathbf{v}_4$ is a spade. In this case, we look for the edge e that is associated with the largest face angle, θ, at the vertex $\mathbf{v}_4$, see Figure 5 (a). Then we contract the edge $\mathbf{v}_1\mathbf{v}_4$ or $\mathbf{v}_2\mathbf{v}_4$ onto $\mathbf{v}_1$ or $\mathbf{v}_2$, respectively, see Figure 5 (b). If none of these contractions is possible, we split $\mathbf{v}_1\mathbf{v}_2$ in its middle point $\mathbf{w}$, see Figure 5 (c), and then we contract the new edge $\mathbf{v}_4\mathbf{w}$ onto $\mathbf{v}_4$, see Figure 5 (d). In this case the splitting of the edge e is always possible, but the contraction of $\mathbf{v}_4\mathbf{w}$ could bring to inverted tetrahedra. If it happens we do not contract the edge $\mathbf{v}_4\mathbf{w}$.

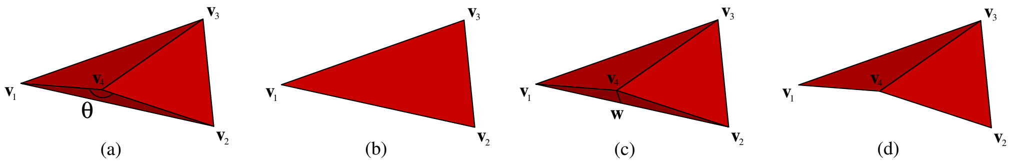

Figure 5: Procedure in the case of spade. In (b) and (d) the faces that could remains in the tetrahedral mesh after the contractions.

3.3 Scheduling of Operations

The inputs of the proposed mesh optimization technique are:

i) an initial tetrahedral mesh;

ii) a threshold value for the quality index, $q_{\min}$;

iii) a threshold value to identify the degenerate tetrahedra, δ;

iv) a maximum number of iterations, N.

Until we reach the maximum number of iteration and we do not find any degenerate tetrahedron, i.e., tetrahedron whose quality index, see Equation 2, is lower than δ, we apply the following work-flow:

1. contraction of wedges, caps and spades;
2. a series of node-smoothing iterations on all the internal vertices of the mesh;
3. contraction of the slivers;
4. a final iteration of node-smoothing on all the internal vertices.

Like all the scheduling proposed in literature even this one is heuristic and it has been developed through a trial and error approach. The result of this mesh improvement procedure is a tetrahedral mesh where all the elements have a quality index greater than the threshold value δ.

3.3.1 Random Operations

We have applied the previous mesh optimization procedure to all the examples proposed in Section 4. We have notice that, after few iterations, the number of degenerate elements drastically decreases. Then, when the optimization procedure tries to improve the quality of the last elements, it could be happen that they disappear or that the number of degenerate tetrahedra remains constant. In fact, the proposed sequence of mesh modification procedure may create a loop of configurations. More precisely we could have a finite sequence of tetrahedra, $\{T_1, T_2, \dots T_m\}$ such that after the first contraction T_1 disappears, but the degenerate tetrahedron T_2 appears. Then, when we remove T_2, the degenerate tetrahedron T_3 is created and so on. Finally, at the removal of T_m, the tetrahedron T_1 appears once again. Consequently we will re-do the same sequence of operations and we do not improve the quality of the mesh.

To avoid these loops, we randomize the operation on degenerate elements after K iterations. More in detail, suppose that T is a degenerate tetrahedron. If we have to operate in it during the first K iterations, we always choose among all the possible operation, the one associated with the highest quality of the tetrahedra involved, see Section 3. But, if we operate on T after the K^{th}-iteration, we simply choose one of the possible operations without taking care about the tetrahedra quality.

For instance, suppose that T is a cap. To improve the quality of the mesh, we have to decide among three different edge contractions, $\mathbf{v}_4\mathbf{v}_1$, $\mathbf{v}_4\mathbf{v}_2$ and $\mathbf{v}_4\mathbf{v}_3$ see Figure 3. Then, if we are dealing with T in one of the first K iterations, we always choose the same edge to collapse, i.e., the edge whose contraction produces the highest quality. But, if we consider T after the K^{th}, we randomly choose one of the possible edges to contract. In this way we break the loop, because we do not always do the same operations.

4 Numerical Results

In this section, we show some numerical examples of our optimization procedure. First of all, we try out the algorithm used to identify the different types of degenerate tetrahedra. Then, some applications are taking into account to prove the effectiveness of the optimization procedure by comparing the number of degenerate tetrahedra and the smallest dihedral angle before and after the process. We also assess the computational time.

In all examples considered, we set:

$$q_{\text{min}} = 0.2\,, \quad \delta = 0.1\,, \quad N = 30 \quad \text{and} \quad K = 10\,.$$

The tests are given for a Intel Core 2 Duo CPU P8400 @ 2.26 GHz processor and 3GB RAM.

4.1 Detection Test

In this first example, we test the detection algorithm. As explained in Subsection 2.1, we subdivide the degenerate tetrahedra into four categories: slivers, caps, wedges and spades. Let us consider a tetrahedron T with three fixed vertices, i.e.,

$$\mathbf{v}_1 = \left(\frac{1}{2}, 0, 0\right)\,,\ \mathbf{v}_2 = \left(-\frac{1}{2}, 0, 0\right)\,,\ \mathbf{v}_3 = \left(0, \frac{\sqrt{3}}{2}, 0\right)\,,$$

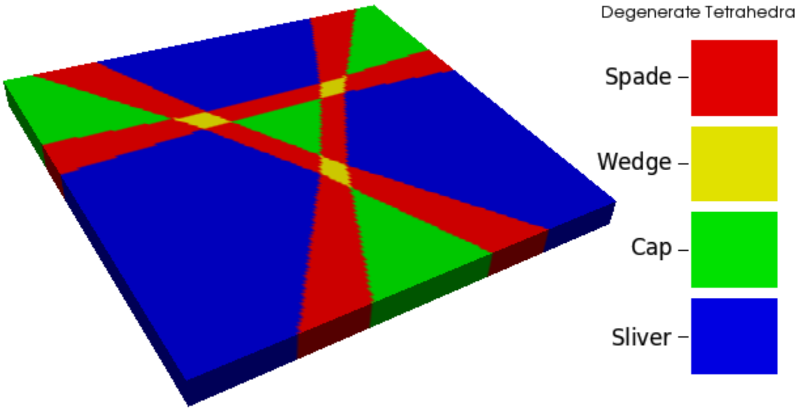

Figure 6: The different types detected.

while we let the fourth one varies over a fixed region. In particular, we consider the family of tetrahedra

$$S = \{\mathbf{v}_1\mathbf{v}_2\mathbf{v}_3\mathbf{v}_4 \,|\, \mathbf{v}_{4,x} \in A_x, \mathbf{v}_{4,y} \in A_y, \mathbf{v}_{4,z} \in A_z\}\,,$$

here $\mathbf{v}_{4,x}$, $\mathbf{v}_{4,y}$, and $\mathbf{v}_{4,z}$ are the x, y and z components of the vertex $\mathbf{v}_4$ and $A_x := [-1.5, 1.5]$, $A_y := [-1, 2]$ and $A_z := [-0.1, 0.1]$. For each tetrahedron in S, we evaluate the degenerate type. As result, we obtain the configuration reported in Figure 6, where each color represents a degenerate tetrahedron type, recalling that the size of the four regions depends on the parameter δ.

We point out that the detection procedure identifies all the possible tetrahedra in S and a tetrahedron in S belongs only to a single class Ω_i.

4.2 Examples

In what follow, the mesh improvement procedure is applied in different test cases. For each example, we show the improved mesh and the initial mesh highlighting the degenerate tetrahedra. Before and after the improvement process, we report the number of tetrahedra, the number of degenerate tetrahedra and the histogram that represents the distribution of the dihedral angle in the range between $0°$ and $20°$. In particular, we indicate the minimum dihedral angle. Finally, we report the number of iterations used, the time employed by the smoothing procedure, the time spent for the collapsing operations and the total time. Compared with *Stellar* [10], the proposed tetrahedral mesh optimization procedure is able to get a final mesh in a lower computational time. In general, we get a final mesh where the minimum dihedral angle is at least $11°$, but *Stellar* could get an astonishing minimum dihedral angles of about $38°$. In Example 1 we consider a parallelepiped divided into three pieces. In Examples 2-3-4-5 we consider the tetrahedral mesh of very complicated mechanical parts. Finally, in Example 6, the proposed optimization algorithm is tested on a real biomedical data. In particular the surface triangular mesh was reconstructed with a Magnetic Resonance Imaging (MRI) technique as described in [4].

5 Conclusions and Future Work

In this paper we have presented a new method to improve the quality of a tetrahedral mesh. In particular, the proposed algorithm applies a specific sequence of local mesh modification procedures for each type of degenerate tetrahedron. Since all the quality indexes proposed in literature detect a low quality tetrahedron, but they do not analyze more in detail its shape, we have developed a new method to identify the type of degenerate tetrahedron.

The reliability and the robustness of this optimization strategy is numerically proved by a large variety of examples. All the test cases show that we got a good quality mesh, i.e. a mesh whose smallest dihedral angle is always more than $11°$. Better results could be obtained by increasing the threshold value of the quality index, δ see Subsection 2.1, but it should be necessary a deeper analysis.

There are a lot of aspects to improve in the proposed method. Firstly, since we desire to preserve the hull and the interfaces of the volume, it could be interesting to make a "ad-hoc" operation for the degenerate tetrahedra that has a face, an edge or a point on the hull of the volume. Moreover, it could be interesting to develop a node-smoothing procedure that involves even the points that lie on the hull and on the interfaces of the domain, see Remark 4.

Finally, since this algorithm consists in local mesh operations, it could lead to a parallel implementation in order to achieve the final high quality mesh in a lower computational time.

Acknowledgements

We gratefully acknowledge Dr. Luciani, Divisione di Cardiochirurgia, Dr. Puppini, Divisione di Radiologia, Ospedale Borgo Trento di Verona and Dr. Faggiano, Politecnico di Milano for the clinical data used in this paper. A special thank to Giudo Francesco Iori for his precious advices on volume tetrahedral meshing.

EXAMPLE 1

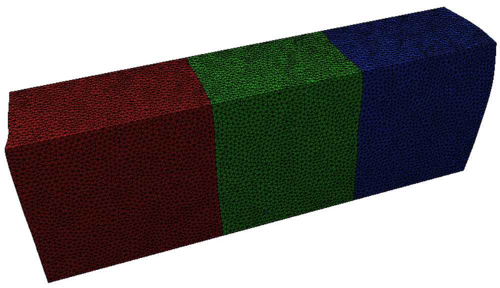

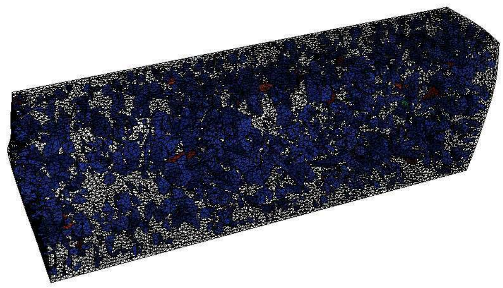

STATISTICS:

BEFORE	AFTER
tets = 68762	tets = 67353
deg. tets = 2516	deg. tets = 0
$\theta_{\text{min}} = 5.00714$	$\theta_{\text{min}} = 11.2843$

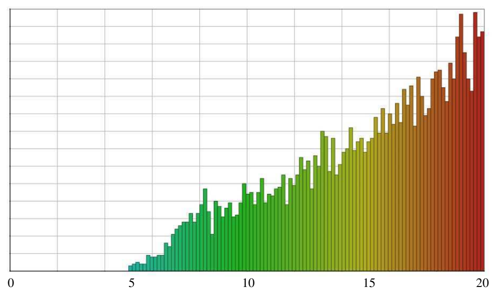

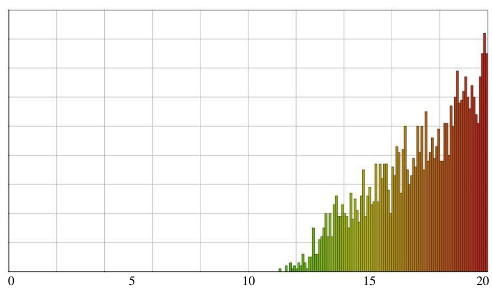

ITERATIONS:	13	SMOOTH TIME:	134 sec.
TOTAL TIME:	170 sec.	COLL TIME:	26 sec.

EXAMPLE 2

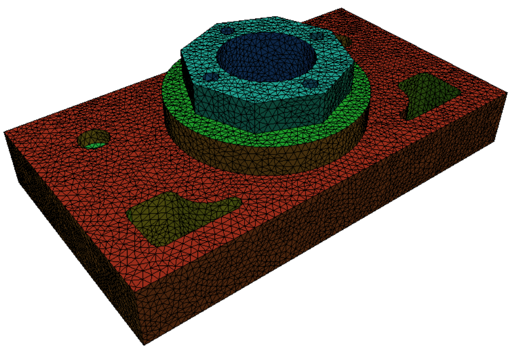

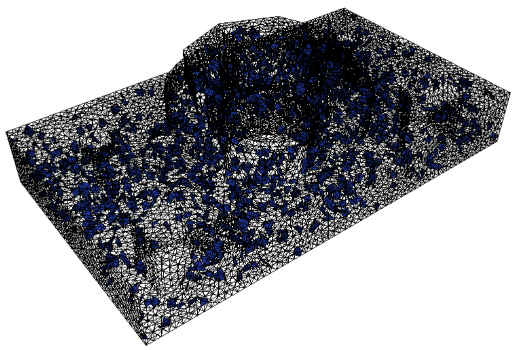

STATISTICS:

BEFORE	AFTER
tets = 164304	tets = 163329
deg. tets = 1867	deg. tets = 0
$\theta_{\min} = 7.96025$	$\theta_{\min} = 12.1735$

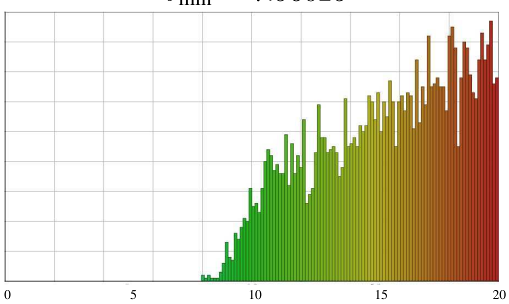

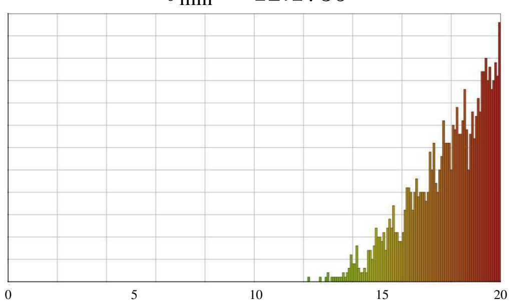

ITERATIONS:	3	SMOOTH TIME:	118 sec.
TOTAL TIME:	138 sec.	COLL TIME:	13 sec.

EXAMPLE 3

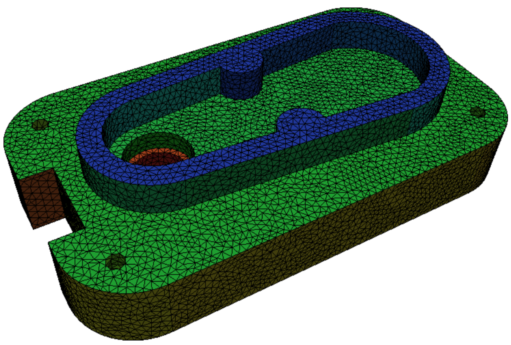

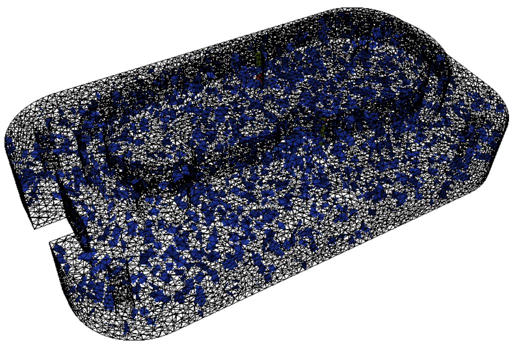

STATISTICS:

BEFORE	AFTER
tets = 167926	tets = 166742
deg. tets = 2173	deg. tets = 0
$\theta_{\min} = 3.33573$	$\theta_{\min} = 12.1167$

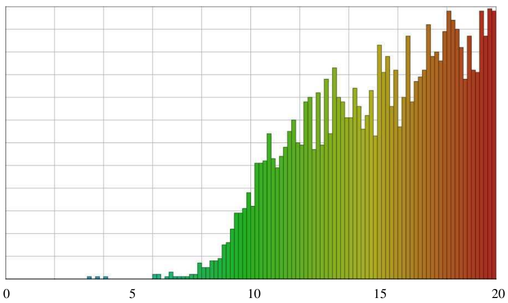

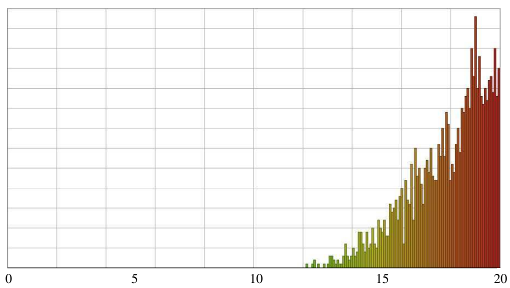

ITERATIONS:	9	SMOOTH TIME:	275 sec.
TOTAL TIME:	334 sec.	COLL TIME:	39 sec.

EXAMPLE 4

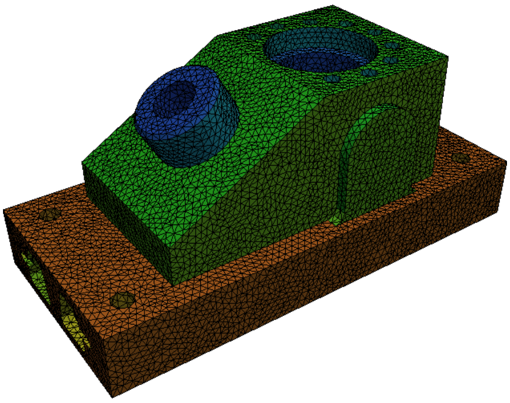

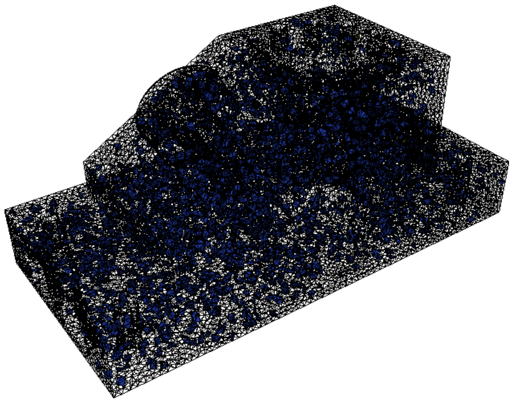

STATISTICS:

BEFORE	AFTER
tets = 368368	tets = 366053
deg. tets = 4529	deg. tets = 0
$\theta_{\min} = 0.633511$	$\theta_{\min} = 12.1436$

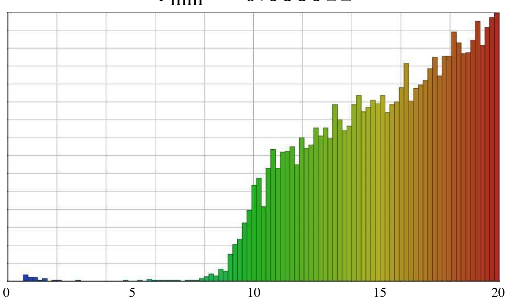

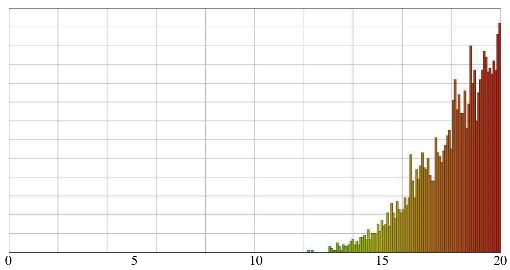

ITERATIONS:	5	SMOOTH TIME:	460 sec.
TOTAL TIME:	531 sec.	COLL TIME:	48 sec.

EXAMPLE 5

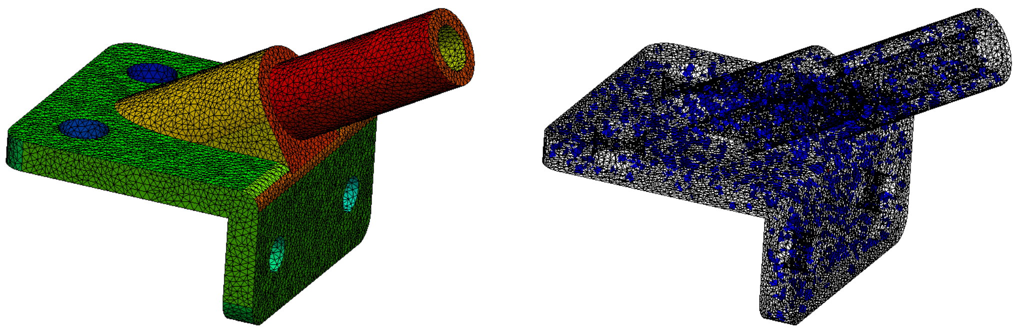

STATISTICS:

BEFORE	AFTER
tets = 135398	tets = 134474
deg. tets = 1566	deg. tets = 0
$\theta_{\min} = 2.77258$	$\theta_{\min} = 12.6567$

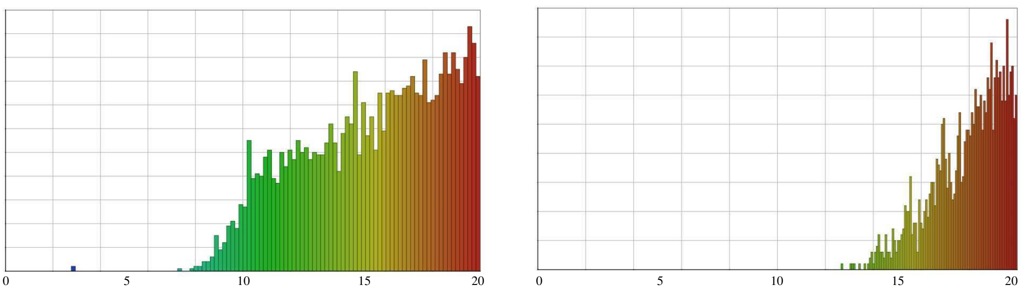

ITERATIONS:	19	SMOOTH TIME:	318 sec.
TOTAL TIME:	397 sec.	COLL TIME:	53 sec.

EXAMPLE 6

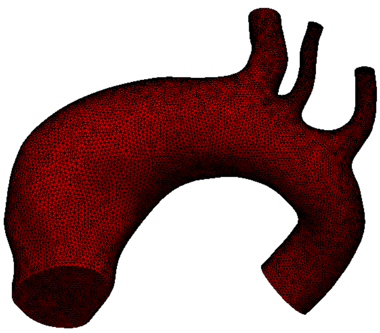

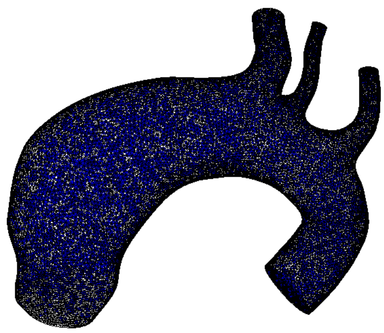

STATISTICS:

BEFORE	AFTER
tets = 1269663	tets = 1264619
deg. tets = 12431	deg. tets = 0
$\theta_{\text{min}} = 6.98889$	$\theta_{\text{min}} = 12.4312$

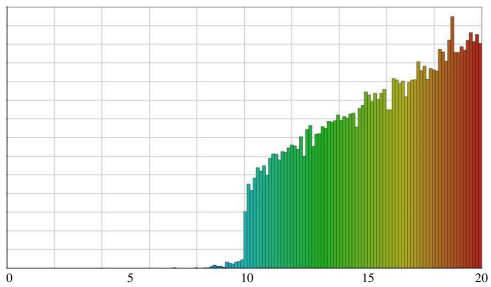

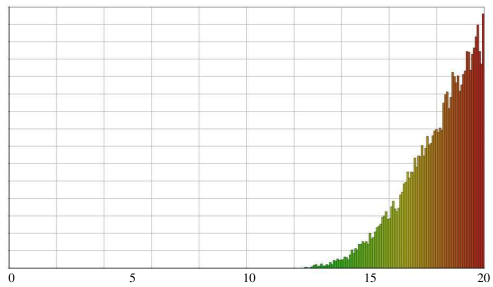

ITERATIONS:	5	SMOOTH TIME:	1030 sec.
TOTAL TIME:	1224 sec.	COLL TIME:	126 sec.

References

[1] Nazmiye Acikgoz and Carlo L Bottasso. Metric-driven mesh optimization using a local simulated annealing algorithm. *International journal for numerical methods in engineering*, 71(2):201–223, 2007.

[2] Carlo L Bottasso. Anisotropic mesh adaption by metric-driven optimization. *International Journal for Numerical Methods in Engineering*, 60(3):597–639, 2004.

[3] Herbert Edelsbrunner and Damrong Guoy. An experimental study of sliver exudation. *Engineering with computers*, 18(3):229–240, 2002.

[4] Elena Faggiano, Luca Antiga, Giovanni Puppini, Alfio Quarteroni, Giovanni Battista Luciani, and Christian Vergara. Helical flows and asymmetry of blood jet in dilated ascending aorta with normally functioning bicuspid valve. *Biomechanics and modeling in mechanobiology*, 12(4):801–813, 2013.

[5] Luca Formaggia and Simona Perotto. Anisotropic error estimates for elliptic problems. *Numerische Mathematik*, 94(1):67–92, 2003.

[6] Lori A Freitag and Patrick M Knupp. Tetrahedral mesh improvement via optimization of the element condition number. *International Journal for Numerical Methods in Engineering*, 53(6):1377–1391, 2002.

[7] Lori A Freitag and Carl Ollivier-Gooch. Tetrahedral mesh improvement using swapping and smoothing. *International Journal for Numerical Methods in Engineering*, 40(21):3979–4002, 1997.

[8] Pascal-Jean Frey and Frédéric Alauzet. Anisotropic mesh adaptation for CFD computations. *Computer methods in applied mechanics and engineering*, 194(48):5068–5082, 2005.

[9] Leonard R Herrmann. Laplacian-isoparametric grid generation scheme. *Journal of the Engineering Mechanics Division*, 102(5):749–907, 1976.

[10] Bryan M. Klingner and Jonathan R. Shewchuk. Agressive tetrahedral mesh improvement. In *Proceedings of the 16th International Meshing Roundtable*, pages 3–23, Seattle, Washington, October 2007.

[11] Gerd Kunert. An a posteriori residual error estimator for the finite element method on anisotropic tetrahedral meshes. *Numerische Mathematik*, 86(3):471–490, 2000.

[12] Jonathan R. Shewchuk. What is a good linear element? interpolation, conditioning, and quality measures. In *Proceedings of 11th International Meshing Roundtable*, pages 115–126, Ithaca, New York, September 2002. Sandia National Laboratories.

MOX Technical Reports, last issues

Dipartimento di Matematica "F. Brioschi",
Politecnico di Milano, Via Bonardi 9 - 20133 Milano (Italy)

14/2014 Dassi, F.; Formaggia, L.; Zonca, S.
Degenerate Tetrahedra Recovering

13/2014 Ballarin, F.; Manzoni, A.; Quarteroni, A.; Rozza, G.
Supremizer stabilization of POD-Galerkin approximation of parametrized Navier-Stokes equations

12/2014 Fumagalli, I; Parolini, N.; Verani, M.
Shape optimization for Stokes flow: a reference domain approach

11/2014 Taddei, T.; Quarteroni, A.; Salsa, S.
An offline-online Riemann solver for one-dimensional systems of conservation laws

10/2014 Antonietti, P.F.; Dedner, A.; Madhavan, P.; Stangalino, S.; Stinner, B.; Verani, M.
High order discontinuous Galerkin methods on surfaces

09/2014 Chen, P.; Quarteroni, A.
A new algorithm for high-dimensional uncertainty quantification problems based on dimension-adaptive and reduced basis methods

08/2014 Cattaneo, L; Zunino, P.
A computational model of drug delivery through microcirculation to compare different tumor treatments

07/2014 Agasisti, T.; Ieva, F.; Paganoni, A.M.
Heterogeneity, school-effects and achievement gaps across Italian regions: further evidence from statistical modeling

06/2014 Benzi, M.; Deparis, S.; Grandperrin, G.; Quarteroni, A.
Parameter estimates for the relaxed dimensional factorization preconditioner and application to hemodynamics

05/2014 Rozza, G.; Koshakji, A.; Quarteroni, A.
Free Form Deformation Techniques Applied to 3D Shape Optimization Problems